In vitro skin model for characterization of sunscreen substantivity upon perspiration

Keshavarzi, Fatemeh; Ø. Knudsen, Nina; Brewer, Jonathan R.; Ebbesen, Morten F.; M. Komjani, Niloufarsadat; Moghaddam, Saeed Z.; Jafarzadeh, Shadi; Thormann, Esben

Published in:
International Journal of Cosmetic Science

Link to article, DOI:
10.1111/ics.12703

Publication date:
2021

Document Version
Peer reviewed version

In vitro skin model for characterization of sunscreen substantivity upon perspiration

Fatemeh Keshavarzi[1,2], Nina Østergaard Knudsen[2], Jonathan R. Brewer[3], Morten F. Ebbesen[3], Niloufarsadat Mirmahdi Komjani[2], Saeed Zajforoushan Moghaddam[1], Shadi Jafarzadeh[2] and Esben Thormann[1*]

[1]Department of Chemistry, Technical University of Denmark, 2800 Kgs. Lyngby, Denmark.

[2] Riemann A/S, Krakasvej 8, 3400 Hillerød, Denmark.

[3] Department of Biochemistry and Molecular Biology, University of Southern Denmark, 5230 Odense M, Denmark.

Corresponding Author:

Esben Thormann

Department of Chemistry, Technical University of Denmark

Address: Kemitorvet, Building 206, Lyngby, 2800 Kgs., Denmark

Tel: +45 45252439

Email: *esth@kemi.dtu.dk

kesha@kemi.dtu.dk

Nina.Knudsen@orkla.dk

brewer@memphys.sdu.dk

mfe@bmb.sdu.dk

This article has been accepted for publication and undergone full peer review but has not been through the copyediting, typesetting, pagination and proofreading process, which may lead to differences between this version and the Version of Record. Please cite this article as doi: 10.1111/ICS.12703

Niloufar.Komjani@orkla.dk

saza@kemi.dtu.dk

shadi.jafarzadeh@orkla.dk

MRS. FATEMEH KESHAVARZI (Orcid ID : 0000-0003-3203-7441)

Article type : Original Article

Abstract

Objective: The resistance of sunscreens to the loss of ultraviolet (UV) protection upon perspiration is important for their practical efficacy. However, this topic is largely overlooked in evaluations of sunscreen substantivity due to the relatively few well-established protocols compared to those for water resistance and mechanical wear.

Methods: In an attempt to achieve a better fundamental understanding of sunscreen behavior in response to sweat exposure, we have developed a perspiring skin simulator, containing a substrate surface that mimics sweating human skin. Using this perspiring skin simulator, we evaluated sunscreen performance upon perspiration by *in vitro* sun protection factor (SPF) measurements, optical microscopy, ultraviolet (UV) reflectance imaging and coherent anti-Stokes Raman scattering (CARS) microscopy.

Results and conclusion: results indicated that perspiration reduced sunscreen efficiency through two mechanisms, namely sunscreen wash-off (impairing the film thickness) and sunscreen redistribution (impairing the film uniformity). Further, we investigated how the sweat rate affected these mechanisms and how sunscreen application dose influenced UV protection upon perspiration. As expected, higher sweat rates led to a large loss of UV-protection, while a larger application dose led to larger amounts of sunscreen being washed-off and redistributed but also provided higher UV protection before and after sweating.

Keywords: sunscreen, substantivity, SPF, perspiring skin simulator, gelatin, sweat resistance.

Introduction

It is well known that sunscreen application is important for the prevention of harmful effects of ultraviolet (UV) radiation on human skin, such as sunburn, photoaging, immunosuppression, and skin cancer.[1–3] Sunscreen is a complex formulation consisting of many ingredients, including UV filters, emollients, and sensory enhancers, film formers, solvents, emulsifiers, and thickeners.[4] UV filters protect against UV irradiation by reflecting, absorbing, or scattering the UV light, and different filters provide the most efficient protection against specific range of light wavelengths (UVB in the wavelength range of 290-320 nm and UVA in the wavelength range of 320-400 nm).[5] A correct combination of UV filters and addition of photostabilizers can enhance the photostability of the final sunscreen product. Emollients, emulsifiers, and solvents are included to ensure the solubility and photostability of the UV filters in the sunscreen.[6] Film formers help the sunscreen film to form a polymeric network on the skin surface that holds and distributes UV filters on the skin to boost the performance of UV filters.[7,8] Thickeners and emulsifiers adjust the viscosity to ensure that the product has good spreadability on the skin and enable the formulation of various forms of sunscreens, such as creams, lotions, sprays, or sticks.[5] An effective sunscreen is optimized with highly photostable (or photostabilized) UV filters that are uniformly spread on the skin to provide broad-spectrum UVB and UVA protection. In addition to optimal protection, substantivity of the product, the ability to bind to the skin and resist removal, is also important for a sunscreen to maintain long-term protection against UV irradiation under real-life conditions.[9,10]

The three main factors used to evaluate sunscreen performance on human skin are the sun protection factor (SPF), UVA protection factor (UVA-PF), and the substantivity.[11] Both SPF and UVA-PF can be measured *in vivo* as the minimum amount of UV energy required to cause a biological endpoint (minimal erythema and persistent pigment darkening, respectively) on sunscreen-treated skin divided by the amount of energy to cause the same effect on unprotected skin. One measure of substantivity is the water resistance test of sunscreen, which is measured by comparing the *in vivo* SPF values of the sunscreen-treated area before and after immersion in water. Moreover, as a means for a rapid, inexpensive, and subject-independent evaluation of formulations and to enable the design of new sunscreen products, *in vitro* SPF, UVA-PF, and water resistance measurements continue to gain more interest.[10–19]

The biological variation of human skin characteristics, such as skin surface topography, may differentially alter the effectiveness of applied sunscreen films.[5,20–26] Furthermore, sweating can alter skin conditions, such as skin surface pH and hydration of the stratum corneum, or even reduce the tolerance of unprotected skin to sunburn.[27][28][29,30] Sweating co-occurs with many conditions in which people use sunscreen, such as exercising outdoors or sunbathing at the beach. This emphasizes that the functionality of sunscreen is important both during and after sweating given that sweating negatively affects sunscreen film homogeneity, substantivity, and consequently reduces the extent of UV protection. The effect of sweating on sunscreen efficacy is often considered to be similar to that of other post-application activities, such as swimming, bathing, and toweling.[9,31,32] However, during perspiration, sweat is released from the skin underneath the film and should be transported across the sunscreen film without impairing its protection, whereas during swimming or toweling the sunscreen film is exposed to water or friction externally and should resist film deterioration or removal. However, sunscreen substantivity is generally assessed by its ability to resist external water exposure or friction while the effect of sweating is commonly overlooked.[21,32–38]

There are few *in vivo* studies investigating the interaction between sweating and sunscreen application, most of which have focused on comparing the water and sweat resistance of sunscreens based on the product formulation.[37,39,40] The importance of sweat resistance in sunscreen was illustrated by studying professional triathletes, who, despite using water resistant sunscreen, were sunburned after competition activities (including swimming, biking, and running), which was possibly due to sunscreen wash-off by sea water and sweating.[41] In another study, the effect of sweat-inducing physical activities on the UV protection of water resistant sunscreens was assessed.[42] While these studies assessed sunscreen film efficacy upon sweating, others investigated the effect of sunscreen film on perspiring conditions, such as skin occlusion or changes in sweat evaporation, skin temperature, and skin cooling.[43–45] *In vivo* evaluations of sunscreen behavior on perspiring human skin are costly, time- and labor-consuming, and complicated due to the intra- and inter-subject biological variability, along with the difficulties in controlling sweat rate and in collection of sweat for analysis. As such, a systematic study evaluating the impact of different parameters, such as sweat rate, sunscreen formulation, and sunscreen application dose, on UV protection properties would face many challenges.[46] To the best of our knowledge, no suitable protocol or *in vitro* method has been

established to enable investigation of the sunscreen/sweat interaction to obtain an improved fundamental understanding of sunscreen behavior and substantivity upon perspiration.

In this study, we developed an *in vitro* setup including a skin-mimicking substrate capable of simulating the perspiration of human skin. Subsequently, this setup, hereafter referred to as the perspiring skin simulator, was used to investigate the performance of an ethanol-based sunscreen formulation both quantitatively and qualitatively by performing *in vitro* SPF measurements and by using an optical microscope and UV reflectance images by an area scan camera, respectively. Moreover, real-time information regarding the interaction between the sweat droplet and the sunscreen film during and after sweating was acquired by coherent anti-Stokes Raman scattering (CARS) microscopy. The *in vitro* SPF measurements and the combination of imaging techniques provided a general knowledge of sunscreen behavior on perspiring skin and enabled us to map the mechanisms of perspiration-induced failure in UV protection. Finally, the effect of two parameters, namely sweat rate and sunscreen application dose, on sunscreen resistance against sweating was investigated.

Materials and methods

Development of the perspiring skin simulator

Materials for skin-mimicking substrate: Gelatin from porcine skin (gel strength ~175 g Bloom, Type A), glycerol (>99.5%), and formaldehyde (ACS reagent, 37% wt. in H_2O, with 10%-15% methanol as a stabilizer) were obtained from Sigma Aldrich (Denmark). Polymethylmethacrylate (PMMA) film (PLEXIGLAS Film 0F058, thickness: 200 µm) was kindly provided by Evonik (Germany). Double-sided acrylic adhesive (Tesa 4900, thickness: 50 µm) was obtained from Tesa (Germany) and track-etched hydrophilic membrane (PCT0220030, pore size: 0.2 µm, pore density: 3×10^8 cm^{-2}, thickness: 10 µm) was obtained from Sterlitech (USA).

To prepare the skin-mimicking substrate, 7.5 g gelatin was mixed with 50 mL water (pH adjusted to 9 with NaOH) and stirred for 30 minutes at 50ºC. 1.5 mL glycerol, as a plasticizer, and 1.5 mL formaldehyde, as a cross-linker, were added and the solution, which was then stirred for one additional minute. The solution was then applied using a casting knife film applicator (Elcometer 3580/4, Elcometer Ltd., UK) with a wet thickness of 250 µm on the PMMA film which was fixed on a vacuum plate (Elcometer 4900, Elcometer Ltd., UK) and left overnight to

dry and cross-link. Prior to film application, the PMMA film was plasma-cleaned (PDC-32G plasma cleaner, Harrick Plasma, USA) for 30 minutes in the air under a constant pressure of 1000 mTorr. This process improves the wettability and adhesion of the PMMA film and consequently prevents delamination of the gelatin layer.[47] After forming a 20-30-µm thick gelatin film, the double-sided acrylic tape was applied from one side to the backside (non-coated side) of the PMMA film while a release liner protected the other side of the tape. Next, funnel-like pores, with a pore density of 200 cm^{-2}, were laser-drilled through the samples using a laser micromachining tool (microSTRUCT™ C, 3D-Micromac AG, Germany). The laser irradiation wavelength, laser power, and marking speed were fixed to 355 nm, 10.5 W, and 400 mm s^{-1}, respectively. This resulted in a pore size of 110-120 µm on the gelatin side and 40-60 µm on the adhesive side. Finally, the release liner of the adhesive was removed and was applied to the track-etched membrane fixed on the vacuum plate. A deadlift of 500 Pa was placed on top of the film for 2 hours to enhance the adhesion of the membrane to the layered system.

The perspiring setup comprises a water tank with adjustable height, a water reservoir under the skin-mimicking surface, a flow sensor (Flow sensor3 digital, FLOW-03D, Elveflow, France), a flow reader (Sensor readerV2, MSR2, Elveflow, France), connecting tubes, and the skin-mimicking substrate. The substrate is placed on the chamber with a lid and an O-ring beneath that fixes the substrate to prevent leakage. The water tank is connected to the chamber to provide pressure-controlled water flow through the substrate and a flow sensor is placed between the water tank and the chamber to measure the flow rate. Figure 1 shows a schematic illustration of the perspiring skin simulator setup. Since salt deposits on the skin mimicking substrate after sweating and subsequent drying will strongly can adsorp and scatter UV light (and thus influence the outcome of SPF measurements), we have in this study chosen to use pure water instead of a saline solution as a representative for sweat.

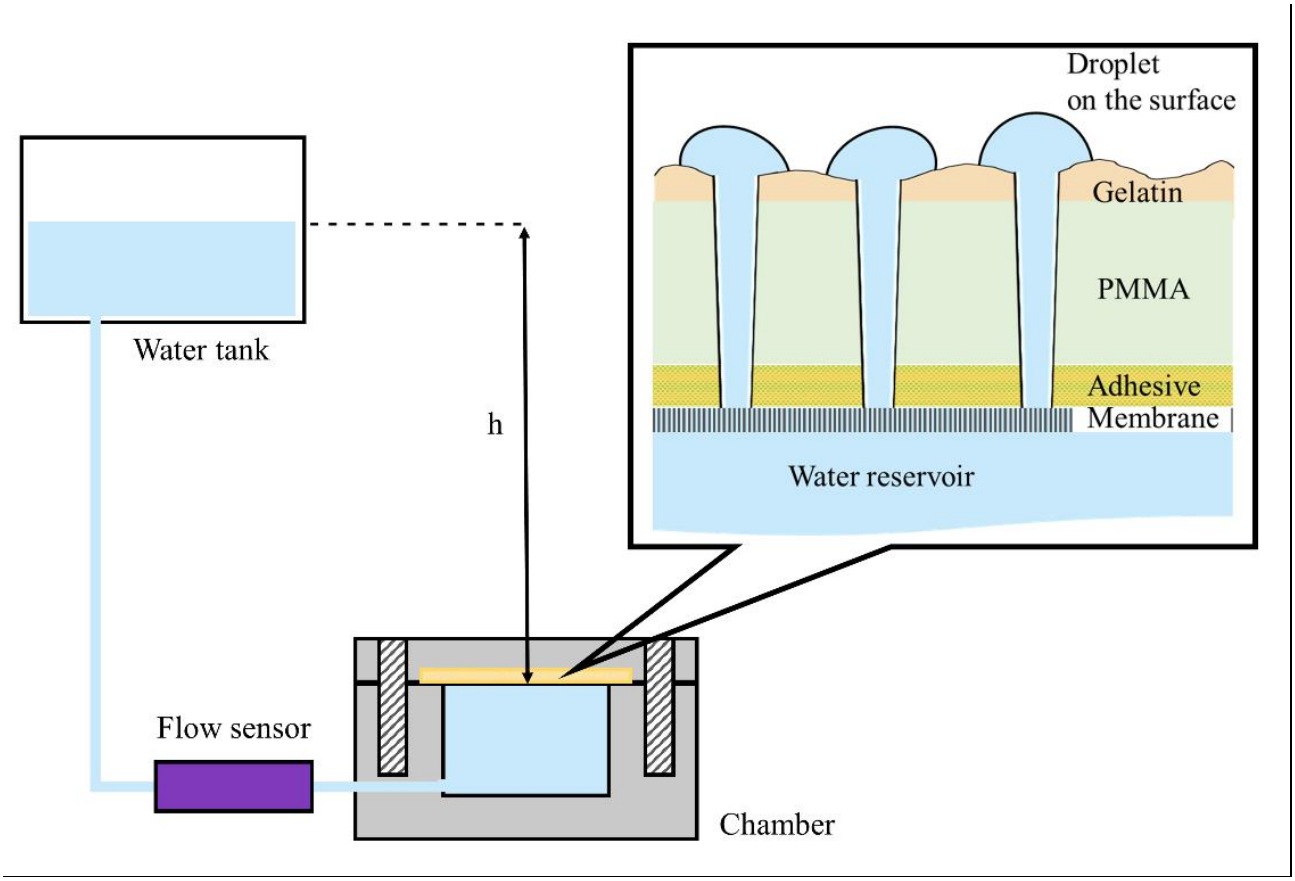

Figure 1. Schematic illustration of the perspiring skin simulator setup and the layered skin-mimicking substrate.

Sunscreen formulations

Materials for sunscreen formulation: Diethylamino hydroxybenzoyl hexyl benzoate (obtained from BASF), octocrylene (obtained from BASF), ethylhexyl salicylate (obtained from DSM Nutritional Products Europe Ltd), C15-19 alkane (obtained from SEPPIC), phenoxyethyl caprylate (obtained from Evonik Nutrition & Care GmbH), acrylate/octylacrylamide copolymer (obtained from Nouryon Surface Chemistry LLC), ethylcellulose (obtained from Ashland), and dibutyl adipate (obtained from BASF) were used as ingredients in the sunscreen formulations evaluated in this study.

Sunscreen was prepared by dissolving the ingredients in ethanol using a homogenizer (Silverson L5T, Silverson Machines Ltd., England) to mimic the main characteristics of an alcohol-based sunscreen. Based on the UV filter composition (diethylamino hydroxybenzoyl hexyl benzoate (10% wt.), octocrylene (10% wt.), and ethylhexyl salicylate (10% wt.)), an SPF of 28 was calculated using a sunscreen simulator software (BASF).[48] Moreover, for CARS microscopy,a

simpler alcohol-based sunscreen formulation containing only one UV filter (20% wt. octocrylene) was prepared following the above-mentioned procedure. This simplified formulation was in order to obtain the stronger CARS signal from octocrylene and in order to avoid overlapping signals from the two UV filters,.

Parameters affecting sunscreen efficacy upon perspiration

Two key parameters, sweat rate and the amount of sunscreen applied, were assessed to investigate their impact on sunscreen substantivity. The sweat rates of 1.46 and 3.31 μL min^{-1} cm^{-2} were selected based on the sweat rates on untreated human foreheads in two different conditions of moderate and heavy sweating.[46] We selected 0.6 and 1.2 mg cm^{-2} as the sunscreen application dose based on the amounts of sunscreen commonly applied by consumers.[49] Accordingly, the following three sets of experiments were conducted: low sunscreen quantity and moderate sweating (0.6 mg cm^{-2} and 1.46 μL min^{-1} cm^{-2}), low sunscreen quantity and heavy sweating (0.6 mg cm^{-2} and 3.31 μL min^{-1} cm^{-2}), and high sunscreen quantity and heavy sweating (1.2 mg cm^{-2} and 3.31 μL min^{-1} cm^{-2}).

***In vitro* measurement of SPF**

In vitro SPF measurements were obtained based on UV transmittance spectroscopy data as follows:

$$SPF = \sum_{290}^{400} E(\lambda)S(\lambda) \Big/ \sum_{290}^{400} E(\lambda)S(\lambda)T(\lambda) \qquad 1$$

where, E(λ) is the erythema action spectrum[50], S(λ) is the spectral irradiance of the UV source, and T(λ) is the measured transmittance of the light through a sunscreen film applied on a UV-transparent substrate. For this, we used a bare skin-mimicking substrate placed on a molded PMMA plate (Helioplates HD6; Helioscreen, Creil, France) as the reference for all SPF measurements. All UV transmittance spectra of the different layers and the skin-mimicking substrate were obtained and have been provided in the supporting information (Figure S1). T(λ) was recorded from 290 to 400 nm through the substrate before and after sunscreen application, as well as after perspiration, using a UV transmittance analyzer (Labsphere UV-2000S, Labsphere Inc., North Sutton, NH, USA). Sunscreen was applied on the substrate using a pipette and distributed homogenously over the whole surface with a latex finger cot pre-saturated with

sunscreen. The sample was allowed to settle for 15 minutes in the dark before the initial SPF measurement. After sweating at room temperature for 20 minutes, the chamber was drained and maintained vertically to off-load excess water on the substrate surface. The sample was then allowed to dry for 20 minutes, after which the skin-mimicking substrate was detached from the chamber and the post-perspiring *in vitro* SPF was measured. For each set of experiments, ten skin-mimicking substrates were examined, and for each substrate, the *in vitro* SPF was measured at nine locations to allow intra-sample comparison of data.

Imaging

An optical microscope (Nikon Eclipse LV100ND optical microscope, Nikon, Japan) was used to visualize sunscreen film distribution on the skin-mimicking substrate before, during, and after perspiration.

An area scan camera (acA4024-29um, Basler AG, Germany) equipped with a UV band-pass filter (365 nm, F/BP365-CMOUNT) and a high-resolution lens (Fujinon HF-1218-12M, Fujifilm, Japan) was used to visualize the distribution of UV filters (specifically with UV absorption at a wavelength of 365 nm) in the sunscreen during perspiration. The chamber was placed in a box equipped with LED UV lamps emitting UVA radiation and the camera was fixed perpendicular to the chamber.

CARS imaging (TCS SP8 CARS microscope, Leica Microsystems, Germany) was initially performed to identify the CARS signals of octocrylene, the simplified sunscreen formulation, and the skin-mimicking substrate. The pump laser (PicoEmerald pump laser, APE, Germany) wavelength varied from 787 to 877 nm with 1-nm increments (wavenumbers ranging from 3313 to 2009 cm^{-1}) with a Stokes laser fixed at 1064 nm. Figure 2a illustrates the chemical bond vibrations of octocrylene. The same wavelength scan was separately performed for the skin-mimicking substrate and the remaining component of the sunscreen (see supporting information, Figure S2). Among the distinguishable peaks of octocrylene (3063, 2864, and 2210 cm^{-1}), the distinct peak at wavenumber 2210 cm^{-1}, attributed to the nitrile group (see Figure 2a), was selected for further studies because it did not overlap with peaks from other ingredients in the sunscreen formulation and the skin-mimicking substrate. As summarized in Figure 2b and 2c, the highest chemical contrast between the sunscreen and the skin-mimicking substrate was visible at wavenumber 2210 cm^{-1}. Figure 2d presents the CARS image of the sunscreen distribution on the

substrate at this wavenumber. Next, sunscreen was applied onto the skin-mimicking substrate at a quantity of 2 mg cm^{-2} (for achieving a higher intensity and therefore better illustration of the sunscreen film on the skin-mimicking substrate) and was maintained in the dark at room temperature for 15 minutes to self-level and dry. The substrate was then mounted on the chamber and the chamber was inversely placed on the sample stage of the microscope to probe the interaction between sweat droplets and the sunscreen film in real-time during and after perspiration. All images were obtained with a field of view of 1550 × 1550 μm^2 at room temperature and image sequences were acquired at 2210 cm^{-1} with a pixel size of 3.033 × 3.033 μm^2.

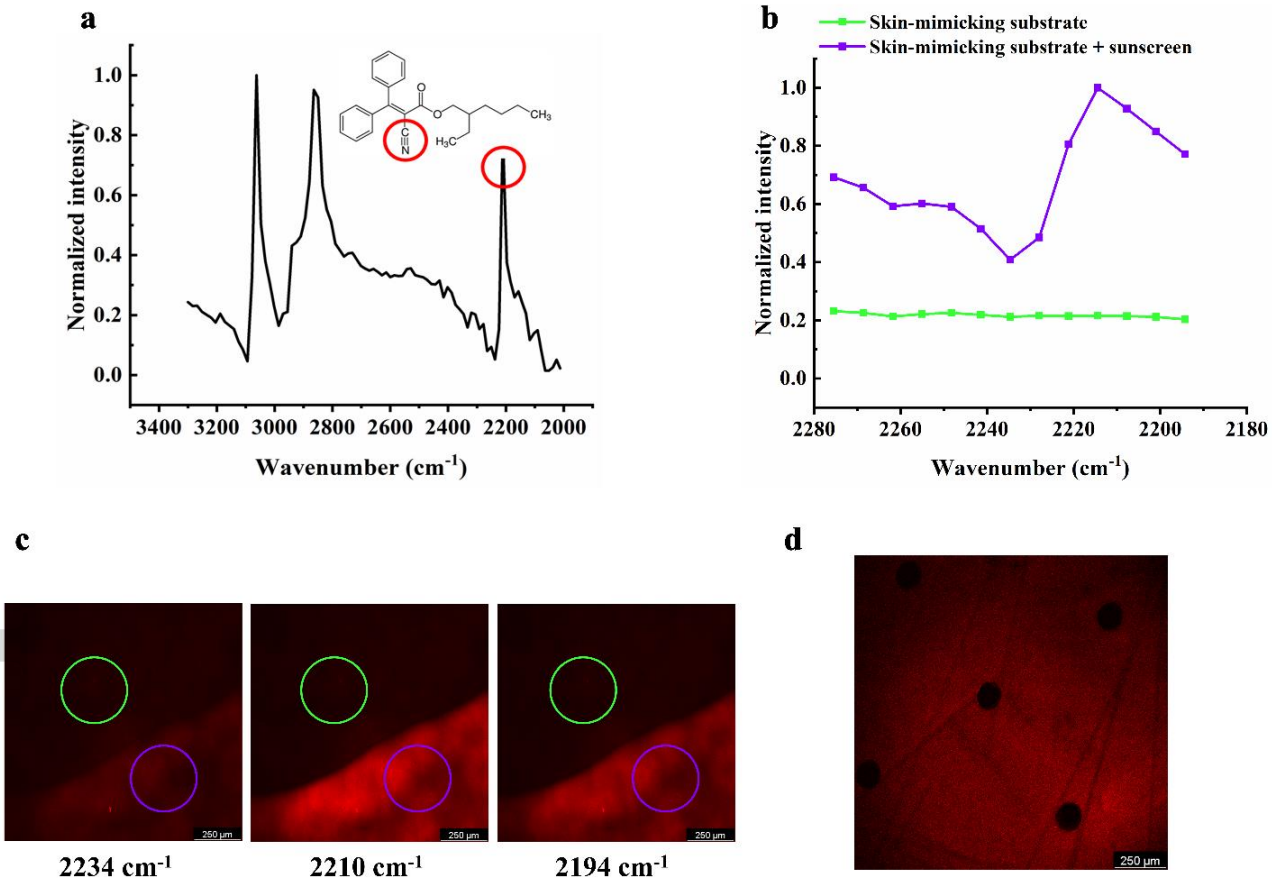

Figure 2. (a) CARS signal for octocrylene from 3300 to 2000 cm^{-1}. The highlighted peak at 2210 cm^{-1} is attributed to the octocrylene nitrile group. (b) CARS signal of the skin-mimicking substrate for two regions: bare substrate (green circle) and area with sunscreen (purple circle). (c) Selected CARS images of the substrate and substrate + sunscreen at 2234, 2210, and 2194 cm^{-1}. The highest contrast between the regions occurred at wavenumber 2210 cm^{-1}. (d) Sunscreen distribution on the skin-mimicking substrate at wavenumber 2210 cm^{-1}. The sunscreen was applied at a quantity of 2 mg cm^{-2}.

Results and Discussion

Perspiring skin simulator

The skin-mimicking substrate consists of four layers, namely a gelatin-based film, a PMMA film, an adhesive layer, and a track-etched membrane (Figure 1), with each providing specific functionality. The outermost layer is the gelatin-based film which is responsible for skin-like properties, e.g., surface hydration, water-responsive behavior, and interaction with topical films.[51–54] The gelatin in this layer is crosslinked by formaldehyde to improve hydrolytic stability, and glycerol is added as a plasticizer to enhance flexibility.[52] The water contact angle of the gelatin-based film was 75°±5° (Figure S3), which is comparable to the data reported for human skin,[52,55] and the thickness of the film is comparable to that of the stratum corneum of human skin (20-30 μm).[56] The PMMA film functions as a support to provide mechanical strength to the substrate. The third layer is a water resistant double-sided adhesive used to attach the above layers to the track-etched membrane, which connects the substrate to the water reservoir. The funnel-like holes through the first three layers of the substrate represent human sweat pores in terms of size and pore density.[57] The membrane, as the bottommost layer, is used to provide a uniform flow to mimic human sweating among all the pores.[58–60] Consequently, by applying specific hydrostatic pressure to the substrate, a uniform, controlled, and reproducible flow is supplied through the pores, as previously described by Hou et al.[58]

Figure 3b shows that experimentally measured sweat rates follow a linear relationship between the applied pressure and the flow rate (Q).[58] Repeated measurements confirmed that a possible reduction in pore size, due to swelling of the hydrated gelatin-based layer, is negligible. Minor variations in substrate thickness result in a distribution in sweat pore sizes. Therefore, to obtain equivalent sweat rates for various skin-mimicking substrates, the applied pressures were varied slightly between individual samples.

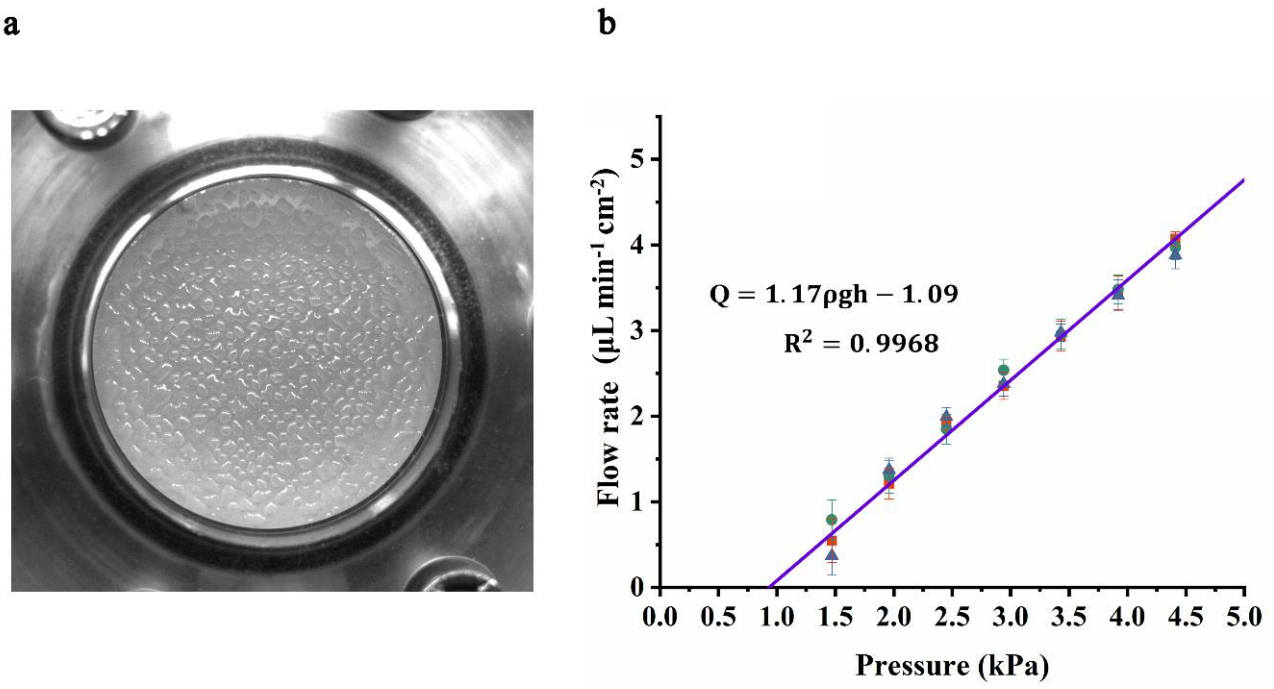

Figure 3. (a) Image of the skin-mimicking substrate during simulated perspiration. (b) Plots of the average sweat rates at different applied pressures. (■) represents the first pressure ramp, (●) shows the first repetition, and (▲) shows the second repetition.

Application of sunscreen to the perspiring skin simulator

An optical microscope was used to visualize the behavior of the sunscreen on the perspiring skin-mimicking substrate. Figure 4a shows the skin-mimicking substrate before sunscreen application. After the application and self-leveling of the sunscreen, a thin and evenly distributed film was formed on the skin-mimicking substrate that also covered most of the sweat pores (Figure 4b). Figure 4c shows the sunscreen-treated substrate after 20 minutes of sweating with a sweat rate corresponding to 3 μL $min^{-1}cm^{-2}$ for uncovered skin (the sweat rate is reduced after sunscreen due to partial occlusion of the pores). Based on the affinity of the sunscreen to the substrate and the film thickness, there is a constant competition between the force of the sweat droplets emerging and the sunscreen film substantivity at different locations. Figure 4d shows the same location as that in Figure 4c, 20 minutes after drying. The sunscreen morphology around the sweat droplets changed and some unprotected areas were observed. Owing to sweat droplet formation and expansion, the sunscreen film is either completely washed-off from the substrate or rearranged on the skin-mimicking surface.

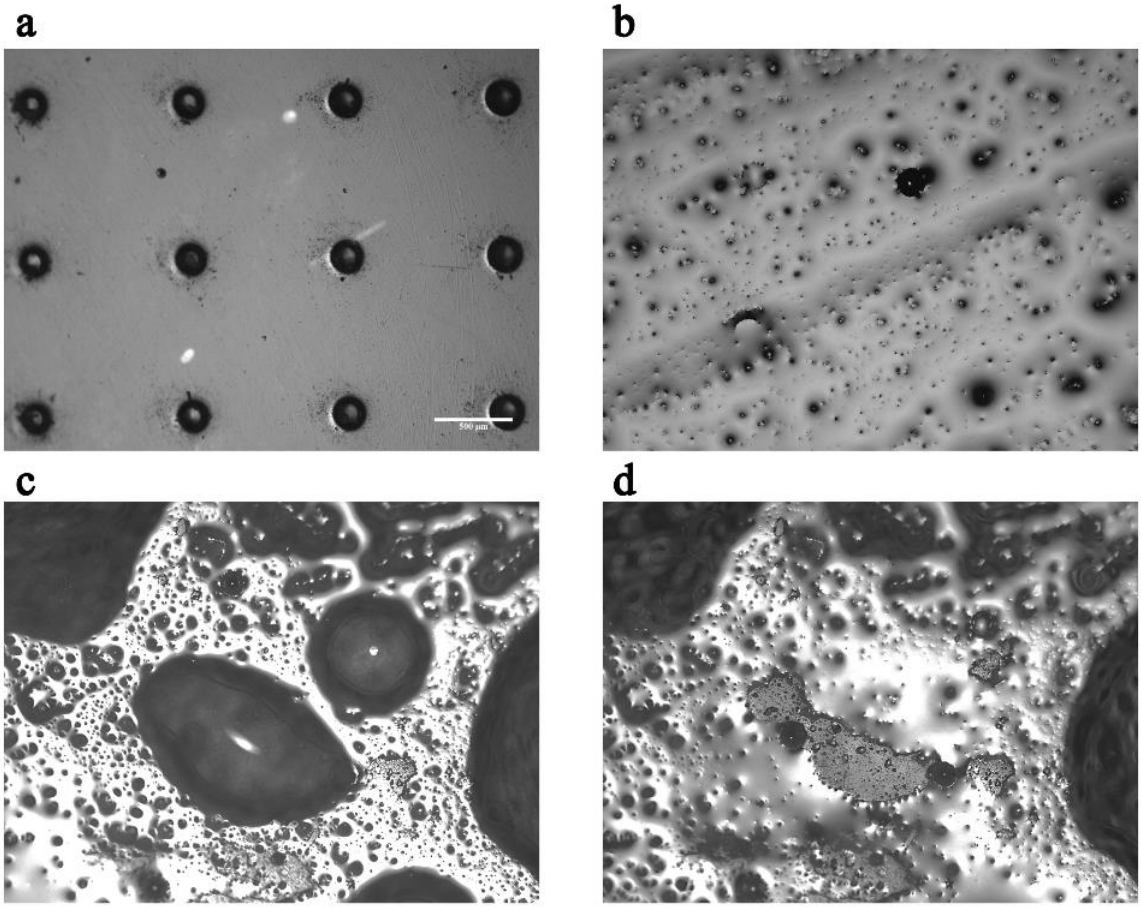

Figure 4. Microscopic images of (a) the bare skin-mimicking substrate, (b) the substrate with sunscreen applied before perspiration, (c) the substrate with sunscreen after 20 minutes of perspiration, and (d) the same spot as in (c), after 20 minutes of drying where the sweat droplet evaporates.

To better observe the potential changes in sunscreen distribution in response to sweating, we utilized a UV reflectance imaging. Here, owing to the specific wavelength of the camera filter, only UVA filters were evaluated. Figure 5a-5d presents UV reflectance images of a sunscreen surface at four stages of sweating on the perspiring skin simulator. The dark areas on the image indicate regions where UV light is absorbed, and a higher intensity of darkness represents a higher concentration of UV filters in that area. Figure 5a shows the uniform distribution of the sunscreen before perspiration was initiated and Figure 5b shows the sweat pores with active perspiration as sweating began. Upon 20 minutes of perspiration, sweat droplets were distributed on the skin substrate (Figure 5c). After drying, the rearrangement of the sunscreen (showing depletion from one spot and accumulation in another) can be observed (Figure 5d). Moreover, some unprotected areas on the skin-mimicking substrate may be attributed to sunscreen wash-off. To highlight the effect of perspiration on sunscreen wash-off, a set of skin-mimicking

substrates were prepared in which only half of the substrate contained sweat pores (Figure 5e). Sunscreen was applied on the area with the sweat pores (Figure 5f) with a quantity of 1.2 mg cm^{-2}. Subsequently, the skin-mimicking substrate was adjusted on the chamber and perspiration began while the chamber was maintained vertically (unlike the other experiments with the perspiring skin simulator where the chamber was in the horizontal position), with the treated area on the upper side. In this manner, during perspiration (for 20 minutes), sunscreen could flow down to the untreated area (Figure 5g). Figure 5h shows the dried skin-mimicking substrate with the visible residue of the washed-off sunscreen on the untreated area. This image also illustrates the redistribution of the UV filters on the treated area. In order to conclude that these observation are similar to effects originating from real sweating situations, we performed a pilot *in vivo* study (see supporting information section S4) that qualitatively demonstrated the same trends when sunscreen was applied on a human forehead and perspiration was induced. Similar observations were also reported in another study of the effect of sweat-inducing physical activities on the UV protection of sunscreens, [42] which then strongly indicates that our observatios are of universal character.

SPF measurements on the skin-mimicking substrate

The *in vitro* SPF measurements of sunscreen applied on the skin-mimicking substrate, before and after exposure to perspiration, were performed to quantify the effect of sweating on the sunscreen film distribution and its UV protection properties. The SPF values were measured at nine locations on each sample (Figure 5i). As an example, pre- and post-perspiration SPF values for a sample with a sunscreen application dose of 0.6 mg cm^{-2} and a sweating rate of 3 μL min^{-1} cm^{-2} are presented in Figure 5j. Here, it can be observed that in all locations, the SPF value decreases in response to perspiration, which is in agreement with the visual observation of decreased film homogeneity.

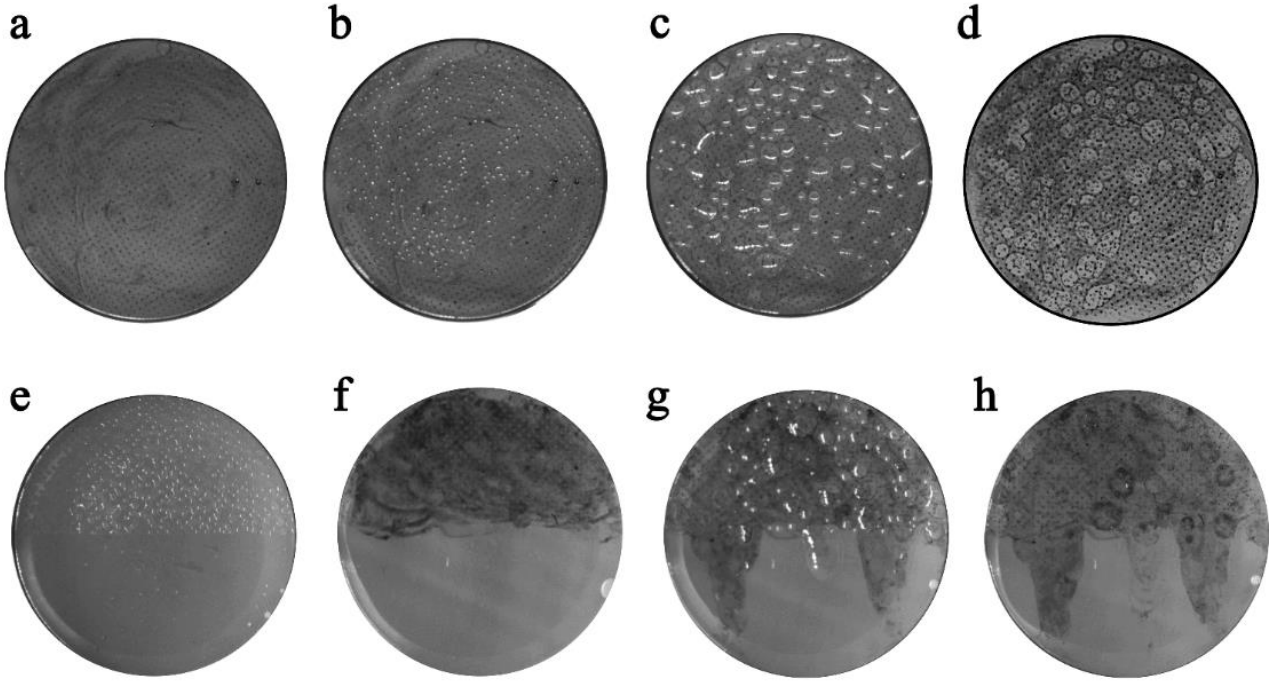

i

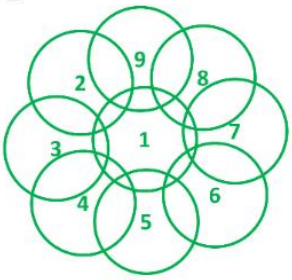

j

Location	1	2	3	4	5	6	7	8	9
SPF (a)	10.3	11.7	12.9	9.0	10.0	8.8	8.4	7.3	10.8
SPF (d)	6.1	7.6	8.1	7.1	6.3	7.7	6.8	5.8	6.4

Figure 5. (a)-(d) UV reflectance images illustrating the sunscreen distribution at different stages: (a) before perspiration, (b) at the beginning of perspiration, (c) after 20 minutes of perspiration, and (d) after 20 minutes of drying. The chamber was kept in horizontal position during the experiment. Darker areas represent higher absorption of UV light. (e)-(h) The skin-mimicking substrate in which only half of the surface could perspire: (e) with activated sweat pores, (f) with sunscreen applied on the area with sweat pores, (g) after perspiring for 20 minutes, and (d) after drying. The chamber was kept in vertical position during the experiment. (i) Locations on the substrate surface used for SPF measurements. (j) SPF measurements for each location before and after perspiration (stages a and d), for a sunscreen with an application dose of 0.6 mg cm^{-2} and a sweating rate of 3 μL $min^{-1}cm^{-2}$.

The optical transmission through an absorbing sunscreen film depends on the film thickness and UV filter concentration, according to the Lambert-Beer law. However, if the film thickness is not uniform, the transmittance will increase regardless of the average thickness, as qualitatively illustrated by a simple step-film-model by O'neill[61] and by other more accurate descriptions of the sunscreen inhomogeneities.[24,62] Therefore, perspiration may differentially affect the sunscreen film; thus, in the present study, we suggest that the reduction in SPF following

perspiration may be described by two main mechanisms, namely direct sunscreen wash-off due to running sweat and redistribution of the sunscreen over the skin surface. To this end, the first mechanism will lead to a decrease in the mass of active ingredients per unit area and thus result in a lower average thickness of the sunscreen film, while the second mechanism will lead to a decreased film homogeneity and thus result in poorer protection.

Imaging the interaction between sweat and sunscreen using CARS microscopy

Real-time probing of the interaction between a sweat droplet and the sunscreen film was characterized by CARS microscopy. Sunscreen containing octocrylene as the only UV filter was applied on the perspiring skin simulator and the UV filter distribution was followed in real-time during perspiration. It was observed that, as the water droplets expanded, the sunscreen film was pushed in the direction of their expansion. Figure 6 shows the octocrylene around an expanding sweat droplet that first expands and then merges with another droplet. The figure shows two cross-sections, one at the surface of the substrate and the other at a location that is 60 μm higher than the substrate. The red halo at the borders of the sweat droplets implies that the UV filter is pushed away radially upon droplet expansion. Next, when active perspiration was stopped and the droplet subsequently evaporated, the thinned layer of sunscreen on the droplet appeared to return to the skin-mimicking surface and formed a different, less uniform morphology compared to the initial film structure. This partial self-healing of the sunscreen layer is shown in Figure 7.

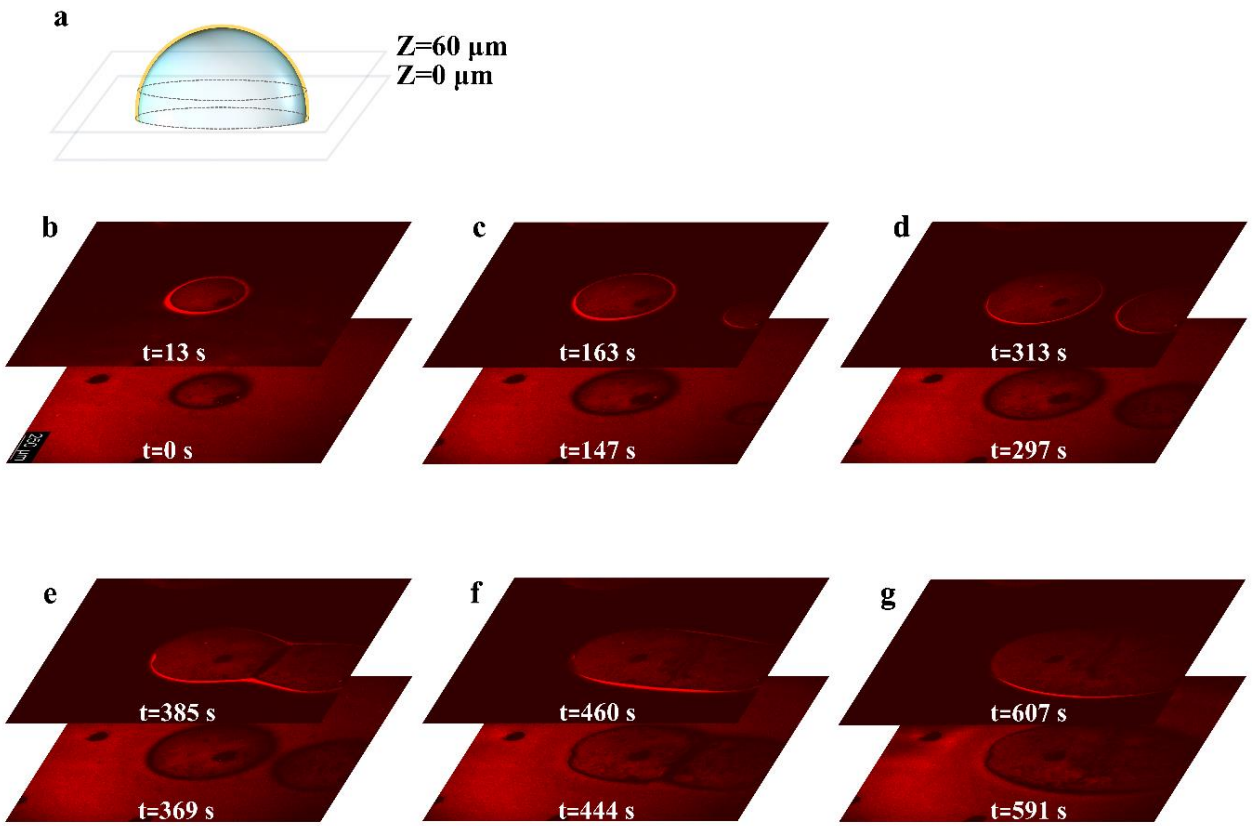

Figure 6. CARS images obtained during sweat droplet growth. (a) A schematic representation of cross-sections of a sweat droplet at the substrate surface, z=0 µm and at a height of z=60 µm. (b-g) Time evolution of sweat droplet growth and merging. As the sweat droplets expand, UV filters are noticeably pushed in the direction of expansion.

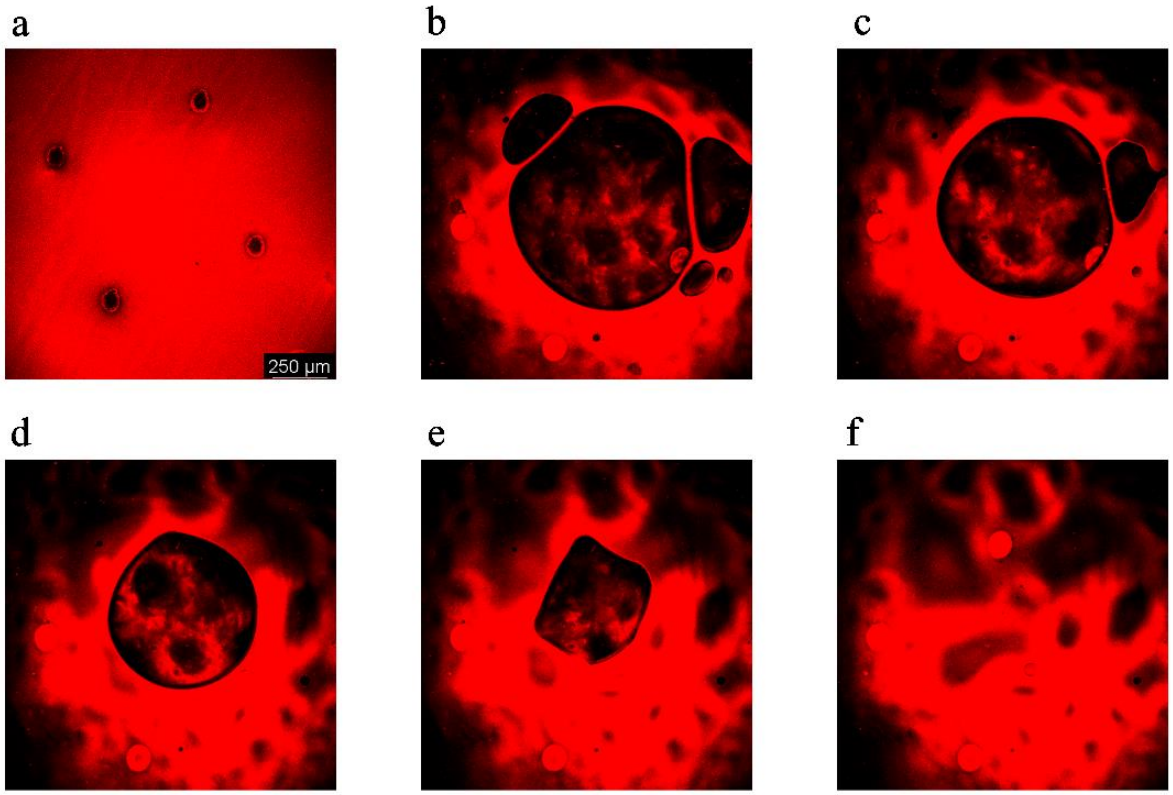

Figure 7. CARS images obtained during the evaporation of a sweat droplet. (a) The initial distribution of UV filters. (b-f). Time evolution of sweat droplet evaporation (t=0, 182, 364, 546, 728 s, respectively).

The data obtained from the combination of different imaging techniques (optical microscopy, UV reflectance imaging, and CARS microscopy) indicate that the pressure from the initial growth of sweat droplets disturbs the homogeneity of the sunscreen film on the skin. As sweating continues, it can lead to relocation of UV filters (impairing the film uniformity) or complete removal of those components of the sunscreen that are poorly attached to the skin substrate (impairing the film thickness). Finally, after perspiration, evaporation of sweat droplets may cause a secondary relocation of UV filters (Figure 7). Taken together, all these actions will affect sunscreen film substantivity and reduce uniform UV protection of the skin in response to perspiration.

Effect of sweat rate and sunscreen amount on sunscreen efficacy

We next investigated the effect of sweat rate and the applied amount of sunscreen on its sweat resistance properties. Figure 8a and 8b show the initial local SPF values and their associated SPF values after sweating at moderate and heavy rates (1.46 and 3.31 µL min^{-1} cm^{-2}, respectively), for

samples with a low application dose of sunscreen (0.6 mg cm^{-2}). The figures provides these values for for nine individual measureing positions (as shown in Figure 5i) obtained on ten replica surfaces (represented by different colours). By this representation one clearly see not only the gereral reduction in SPF (due to sunscreen wash-off) but also the large position dependent variations within each sample (due to sunscreen redistribution).

For both moderate and heavy sweating, results indeed indicated a general trend of decreasing SPF in response to perspiration. However, for some local spots, the SPF increased or did not change or even increased. Especially, at the lower sweat rate, the SPF values after perspiration demonstrated large position dependens compared to the samples exposed to higher sweat rates. Based on the UV reflectance images (supporting information, Figure S5), at high sweat rates, the sweat droplets merge and form larger droplets, thereby increasing the possibility of sunscreen wash-off. In contrast, at the low sweat rate, the sweat droplets do not propagate extensively, resulting in less sunscreen wash-off from the surface.

Next, studying how the sunscreen application doses (0.6 and 1.2 mg cm^{-2}, respectively) affected the substantivity with respect to sweating (Figure 8c), unsurprisingly revealed that the SPF reduction was higher when a higher amount of sunscreen was applied (simply because more sunscreen can be washed-off and redistributed). However, it should be noted that because the initial SPF values for the samples with a higher application dose of sunscreen were much higher than those of the samples with a lower application dose of sunscreen, the absolut SPF values are still higher when a higher sunscreen dose is applied (ses supporting information, Figure S6 and S7 for more details).[63,64]. This observation is further in agreenment with UV reflectance images indicated that the low amount of applied sunscreen resulted in more unprotected areas during similar perspiration conditions (supporting information, Figure S8).

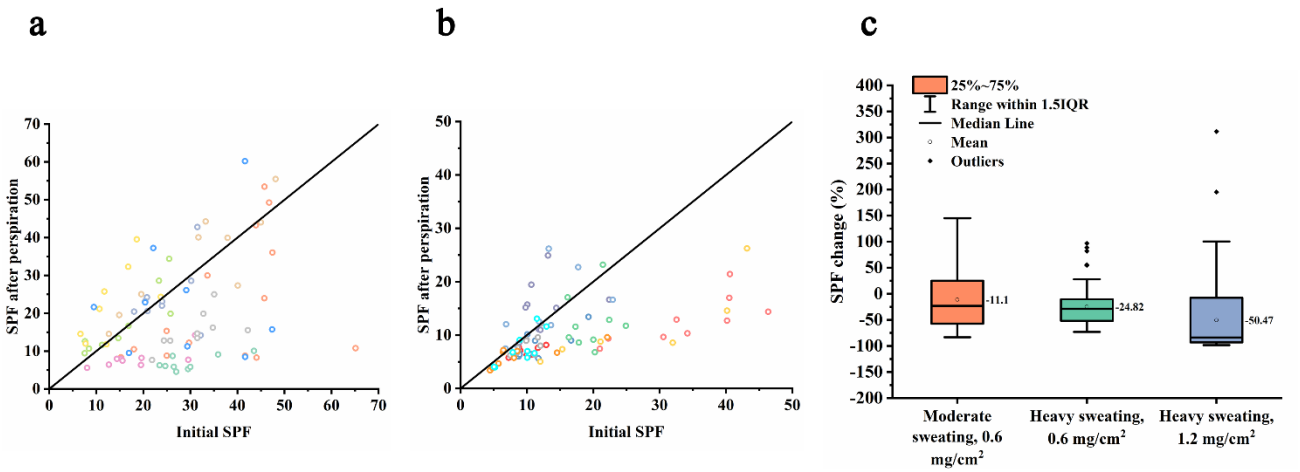

Figure 8. Initial versus final SPF values for a low amount of applied sunscreen (0.6 mg cm^{-2}) with (a) moderate sweating (1.46 µL $min^{-1}cm^{-2}$) and (b) heavy sweating (3.31 µL $min^{-1}cm^{-2}$). Each color represents nine locations on an individual sample. The solid line represents the location of the data point if no effect of sweating was observed and the data point layer below the line thus represents a situation where the SPF values decreased. (c) Statistical representation of the differences in measured SPF before and after perspiration. The colored area represents the interquartile range (IQR) showing the range of middle 50% of the data (25% to 75%). The middle line represents the median and the small square represents the mean value. The mean value for each set of experiments is shown beside each boxplot. The upper and lower lines represent the maximum and minimum SPF changes, respectively, excluding the outliers. The rhombuses outside the box indicate outliers.

We also measured the UVA/UVB ratio and the critical wavelength (λ_c) on the tested samples, as these parameters might provide additional information on the intensity of UV absorption over specific regions of the spectrum. Comparison of these two factors before and after perspiration may illustrate which of the UVA and UVB filters are more prone to wash-off. Results indicated negligible changes upon both moderate and heavy sweating (Supporting information, Figure S9), thereby implying that both UVA and UVB filters underwent comparable changes in our studied formulation.[65] Similarly, λ_c did not change upon perspiration (Supporting information, Table S1). However, depending on the selected UV filters in a given sunscreen formulation, results may vary. [65,66]

Conclusion

We have developed a perspiring skin simulator that includes a multilayer skin-mimicking substrate and presents a new *in vitro* method to evaluate sunscreen substantivity upon perspiration. This setup mimics sweating human skin in terms of sweat pore size, sweat pore density, sweat rate, and skin-like affinity for sunscreen products. Our results demonstrated that

sweating diminished sunscreen efficacy by impairing the sunscreen thickness and uniformity. More specifically, sweating reduced the SPF via both sunscreen wash-off and sunscreen redistribution. Different imaging techniques used in this study (optical microscopy, UV reflectance imaging, and CARS microscopy) illustrated that the sweat droplet formation negatively affects the uniformity of sunscreen film, as well as the distribution of UV filters presented in the film. Moreover, the CARS microscopy images obtained during evaporation of sweat droplets show a secondary redistribution of UV filters and partial self-healing of the sunscreen layer. Although this was observed for one specific sunscreen formulation, we expect this observation to be generalizable. Finally, the model was employed to demonstrate how different sweat rates and sunscreen application doses affect sunscreen performance. This study implies that higher sweat rates lead to lower substantivity, while a larger application dose can be used to achieve higher post-perspiration UV protection. After implementation of this novel method for *in vitro* characterization of sunscreen performance, future studies should focus on the influence of sunscreen formulation and sweat composition.

References

1. Schalka S, Manoel V. Sun Protection Fator: meaning and controversies. An Bras Dermatol. 2011;86(3):507–15.
2. Olsen CM, Wilson LF, Green AC, Biswas N, Loyalka J, Whiteman DC. Prevention of DNA damage in human skin by topical sunscreens. Photodermatol Photoimmunol Photomed. 2017;33(3):135–42.
3. Li H, Colantonio S, Dawson A, Lin X, Beecker J. Sunscreen Application, Safety, and Sun Protection: The Evidence. J Cutan Med Surg. 2019;23(4):357 –369.
4. Osterwalder U, Sohn M, Herzog B. Global state of sunscreens. Photodermatol Photoimmunol Photomed. 2014;30(2–3):62–80.
5. Tanner PR. Sunscreen product formulation. Dermatol Clin. 2006;24(1):53–62.
6. Sohn M, Amorós-Galicia L, Krus S, Martin K, Herzog B. Effect of emollients on UV filter absorbance and sunscreen efficiency. J Photochem Photobiol B Biol. 2020;205(111818):1–8.

7. Davis JA, Petersen D, Li D. Use of film-forming polymers for increased efficacy in sunscreens. J Cosmet Sci. 2007;568–9.

8. Sohn M. UV Booster and Photoprotection. In: Principles and Practice of Photoprotection. 2016. p. 227–45.

9. Latha MS, Martis J, Shobha V, Shinde RS, Bangera S, Krishnankutty B, et al. Sunscreening agents: A review. J Clin Aesthet Dermatol. 2013;6(1):16–26.

10. Rezende SG, Dourado JG, Amorim De Lino FM, Vinhal DC, Silva EC, Gil EDS. Methods used in evaluation of the sun protection factor of sunscreens. Rev Eletrônica Farmácia. 2014;11(2):37–54.

11. Sohn M, Malburet C, Caliskan G, Büchse A, Grumelard J, Chambert M, et al. In vitro water resistance testing using SPF simulation based on spectroscopic analysis of rinsed sunscreens. Int J Cosmet Sci. 2018;40(3):217–25.

12. Brown S, Diffey BL. The effect of applied thickness on sunscreen protection: in vivo and in vitro studies. Phorochemistry ond Photobiol. 1986;44(4):509–13.

13. ROBERT M. SAYRE, AGIN PP, LEVEE GJ, MARUIW E. A comparison of in vivo and in vitro testing of sunscreening formulas. 1979;29.

14. Miksa S, Lutz D, Ongenaed J, Candau D. Adjusting Substrate/Product Interfacial Properties to Improve In vivo/In vitro SPF Correlation. Cosmetics & Toiletries magazine; 2013. p. 170–81.

15. Miksa S, Lutz D, Guy C. New approach for a reliable in vitro sun protection factor method Part I: Principle and mathematical aspects. Int J Cosmet Sci. 2015;37(6):555–66.

16. Pissavini M, Alard V, Heinrich U, Jenni K, Perier V, Tournier V, et al. In vitro assessment of water resistance of sun care products: A reproducible and optimized in vitro test method. Int J Cosmet Sci. 2007;29(6):451–60.

17. Ahn S, Yang H, Lee H, Moon S, Chang I. Alternative evaluation method in vitro for the water-resistant effect of sunscreen products. Ski Res Technol. 2008;14(2):187–91.

18. Santos Caetano JP, Abarca AP, Guerato M, Guerra L, Schalka S, Perez Simão DC, et al. SPF and UVA-PF sunscreen evaluation: are there good correlations among results obtained in vivo, in vitro and in a theoretical Sunscreen Simulator? A real-life exercise. Int J Cosmet Sci. 2016;38(6):576–80.

19. COLIPA. Method for In Vitro Determination of UVA Protection, 2011, COLIPA (European

Cosmetic, Toiletry and Perfumery Association). In Vitro Method for the Determination of the UVA Protection Factor and "Critical Wavelength" Values of Sunscreen Products. Guidelines. 2011;29.

20. Azurdia RM, Pagliaro JA, Diffey BL, Rhodes LE. Sunscreen application by photosensitive patients is inadequate for protection. Br J Dermatol. 1999;140(2):255–8.

21. Petersen B, Wulf HC. Application of sunscreen - theory and reality. Photodermatol Photoimmunol Photomed. 2014;30(2–3):96–101.

22. Neale R, Williams G, Green A. Application patterns among participants randomized to daily sunscreen use in a skin cancer prevention trial. Arch Dermatol. 2002;138(10):1319–25.

23. Holman DM, Berkowitz Z, Guy GP, Hawkins NA, Saraiya M, Watson M. Patterns of sunscreen use on the face and other exposed skin among US adults. J Am Acad Dermatol. 2015;73(1):83–92.

24. Sohn M, Hêche A, Herzog B, Imanidis G. Film thickness frequency distribution of different vehicles determines sunscreen efficacy. J Biomed Opt. 2014;19(11):115005-1-115005–11.

25. Kaidbey KH, Kligman AM. An appraisal of the efficacy and substantivity of the new high-potency sunscreens. J Am Acad Dermatol. 1981;4(5):566–70.

26. Korn V, Surber C, Imanidis G. Skin Surface Topography and Texture Analysis of Sun-Exposed Body Sites in View of Sunscreen Application. Skin Pharmacol Physiol. 2017;29(6):291–9.

27. Kuht J, Farmery AD. Body temperature and its regulation. Vol. 19, Anaesthesia and Intensive Care Medicine. 2018. p. 507–12.

28. Park DH, Park BJ, Kim JM. Hydrochromic Approaches to Mapping Human Sweat Pores. Acc Chem Res. 2016;49(6):1211–22.

29. Wang S, Zhang G, Meng H, Li L. Effect of Exercise-induced sweating on facial sebum, stratum corneum hydration, and skin surface ph in normal population. Ski Res Technol. 2013;19(1):312–7.

30. Moehrle M, Koehle W, Dietz K, Lischka G. Reduction of minimal erythema dose by sweating. Photodermatol Photoimmunol Photomed. 2000;16(6):260–2.

31. Puccetti G, Fares H. A new approach for evaluating the water resistance of sunscreens on consumers: Tap water vs. salt water vs. chlorine water. Int J Cosmet Sci. 2014;36(3):284–90.

32. Poh Agin P. Water resistance and extended wear sunscreens. Dermatol Clin. 2006;24(1):75–9.

33. Kluschke F, Weigmann HJ, Schanzer S, Meinke M, Vergou T, Sterry W, et al. Gain or loss? sunscreen efficiency after cosmetic pretreatment of the skin. Skin Pharmacol Physiol. 2014;27(2):82–9.

34. Bodekær M, Faurschou A, Philipsen PA, Wulf HC. Sun protection factor persistence during a day with physical activity and bathing. Photodermatol Photoimmunol Photomed. 2008;24(6):296–300.

35. Stokes RP, Diffey BL. A novel ex vivo technique to assess the sand/rub resistance of sunscreen products. Int J Cosmet Sci. 2000;22(5):329–34.

36. Wright MW, Wright ST, Wagner RF. Mechanisms of sunscreen failure. J Am Acad Dermatol. 2001;44(5):781–4.

37. Leroy D, Dompmartin A. Sunscreen substantivity - comparison between water and sweat resistance tests. Photodermatology. 1988;5(1):49–50.

38. Diffey BL. When should sunscreen be reapplied? J Am Acad Dermatol. 2001;45(6):882–5.

39. Giese AC, Wells JM. Sweat- and Water-Resistant Sunburn Preparations. J Am Pharm Assoc. 1946;208–12.

40. Korting HC, Schöllmann C. Resistance of liposomal sunscreen formulations against plain water as well as salt water exposure and perspiration. Skin Pharmacol Physiol. 2010;24(1):36–43.

41. Moehrle M. Ultraviolet exposure in the Ironman triathlon. Med Sci Sports Exerc. 2001;33(8):1385–6.

42. Ruvolo E, Aeschliman L, Cole C. Evaluation of sunscreen efficacy over time and re-application using hybrid diffuse reflectance spectroscopy. Photodermatol Photoimmunol Photomed. 2020;(February):1–8.

43. Ou-Yang H, Meyer K, Houser T, Grove G. Sunscreen formulations do not interfere with sweat cooling during exercise. Int J Cosmet Sci. 2017;40:87–92.

44. Connolly DAJ, Wilcox AR. The effects of an application of suncream on selected physiological variables during exercise in the heat. J Sport Med Phys Fit. 2000;40(1):35–40.

45. Aburto-Corona J, Aragón-Vargas L. Sunscreen use and sweat production in men and women. J Athl Train. 2016;51(9):696–700.

46. Taylor NA, Machado-Moreira CA, Sato K, Leidal R, Sato F, Kuno Y, et al. Regional variations in transepidermal water loss, eccrine sweat gland density, sweat secretion rates and electrolyte

composition in resting and exercising humans. Extrem Physiol Med. 2013;2(1):4.

47. Pawde SM, Deshmukh K. Surface Characterization of Air Plasma Treated Poly Vinylidene Fluoride and Poly Methyl Methacrylate Films. Polym Eng Sci. 2009;49(4):808–18.

48. https://www.sunscreensimulator.basf.com/.

49. Bimczok R, Gers-Barlag H, Mundt C, Klette E, Bielfeldt S, Rudolph T, et al. Influence of applied quantity of sunscreen products on the sun protection factor - A multicenter study organized by the DGK Task Force Sun Protection. Skin Pharmacol Physiol. 2007;20(1):57–64.

50. Webb AR, Slaper H, Koepke P, Schmalwieser AW. Know your standard: Clarifying the CIE erythema action spectrum. Photochem Photobiol. 2011;87(2):483–6.

51. Dąbrowska A, Rotaru GM, Spano F, Affolter C, Fortunato G, Lehmann S, et al. A water-responsive, gelatine-based human skin model. Tribol Int. 2017;113:316–22.

52. Lir I, Haber M, Dodiuk-Kenig H. Skin surface model material as a substrate for adhesion-to-skin testing. J Adhes Sci Technol. 2007;21(15):1497–512.

53. Bhushan Bharat, Tang W. Surface, Tribological, and Mechanical Characterization of Synthetic Skins for Tribological Applications in Cosmetic Science. J Appl Polym Sci. 2011;120(7):2881–90.

54. Keshavarzi F, Zajforoushan Moghaddam S, Barré Pedersen M, Østergaard Knudsen N, Jafarzadeh S, Thormann E. Water vapor permeation through topical films on a moisture-releasing skin Model. Ski Res Technol. 2020;00:1–10.

55. Gerhardt LC, Schiller A, Müller B, Spencer ND, Derler S. Fabrication, characterisation and tribological investigation of artificial skin surface lipid films. Tribol Lett. 2009;34(2):81–93.

56. Yuan Y, Verma R. Measuring microelastic properties of stratum corneum. Colloids Surfaces B Biointerfaces. 2006;48(1):6–12.

57. Chen X, Gasecka P, Formanek F, Galey JB, Rigneault H. In vivo single human sweat gland activity monitoring using coherent anti-Stokes Raman scattering and two-photon excited autofluorescence microscopy. Br J Dermatol. 2016;174(4):803–12.

58. Hou L, Hagen J, Wang X, Papautsky I, Naik R, Kelley-Loughnane N, et al. Artificial microfluidic skin for in vitro perspiration simulation and testing. Lab Chip. 2013;13(10):1868–75.

59. Hansen D, Zajforoushan Moghaddam S, Eiler J, Hansen K, Thormann E. Performance of Polymeric Skin Adhesives during Perspiration. ACS Appl Polym Mater. 2020;2(4):1535–42.

60. Eiler J, Hansen D, Bingöl B, Hansen K, Heikenfeld J, Thormann E. In vitro evaluation of skin adhesives during perspiration. Int J Adhes Adhes. 2020;99(102574):1–7.

61. O'neill JJ. Effects of film irregularities on sunscreen. Joural Pharm Sci. 1983;73:888–91.

62. Herzog B. Models for the Calculation of Sun Protection Factors and Parameters Characterizing the UVA Protection Ability of Cosmetic Sunscreens. Vol. 4, Colloids and Interface Science Series. 2010. 275–308 p.

63. Ferrero L, Pissavini M, Doucet O. How a calculated model of sunscreen film geometry can explain in vitro and in vivo SPF variation. Photochem Photobiol Sci. 2010;9(4):540.

64. Sohn M, Malburet C, Baptiste L, Prigl Y. Development of a Synthetic Substrate for the in vitro Performance Testing of Sunscreens. Skin Pharmacol Physiol. 2017;30(3):159–70.

65. Stokes RP, Diffey BL, Dawson LC, Barton SP. A novel in vitro technique for measuring the water resistance of sunscreens. Int J Cosmet Sci. 1998;20(4):235–40.

66. Stokes RP, Diffey BL. The water resistance of sunscreen and day-care products. Br J Dermatol. 1999;140:259–63.